

# Towards a robotic model of the mirror neuron system

Kristína Rebrová, Matej Pecháč & Igor Farkaš  
 Faculty of Mathematics, Physics and Informatics  
 Comenius University in Bratislava  
 Mlynská dolina, 84248 Bratislava, Slovak Republic  
 Email: {rebrova,farkas}@fmph.uniba.sk

**Abstract**—Action understanding undoubtedly involves visual representations. However, linking the observed action with the respective motor category might facilitate processing and provide us with the mechanism to “step into the shoes” of the observed agent. Such principle might be very useful also for a cognitive robot allowing it to link the observed action with its own motor repertoire in order to understand the observed scene. A recent account on action understanding based on computational modeling methodology suggests that it depends on mutual interaction between visual and motor areas. We present a multi-layer connectionist model of action understanding circuitry and mirror neurons, emphasizing the bidirectional activation flow between visual and motor areas. To accomplish the mapping between two high-level modal representations we developed a bidirectional activation-based learning algorithm inspired by a supervised, biologically plausible GeneRec algorithm. We implemented our model in a simulated iCub robot that learns a grasping task. Within two experiments we show the function of the two topmost layers of our model. We also discuss further steps to be done to extend the functionality of our model.

**Keywords**—action understanding, mirror neurons, cognitive robotics, iCub, neural network

## I. INTRODUCTION

Action understanding is one of the crucial capacities of human and animal cognition. In line with embodied cognition and the claim that cognition is for action [1], it is very important to study how the sensorimotor circuitry works in animals and humans and how it is related to one’s understanding of the surrounding world. Among the theories aiming to explain the nature of action understanding and its neural correlates, two rival theories can be distinguished [2]. According to *the visual hypothesis*, the observed action is assessed solely on the basis of visual processing and is hence mediated by visual areas of the brain. On the contrary, *the direct matching hypothesis* emphasizes the involvement of motor modality, namely the mapping of the observed action onto an action in one’s own motor repertoire and back, to complete visual information processing. This observation–execution matching property has been found in *mirror neurons*. Endowing a humanoid robot with mirror neuron circuitry might be a valuable step towards action understanding in cognitive robotics and in human–robot interaction.

### A. Mirror neurons and action understanding

Mirror neurons were originally discovered in area F5 (responsive to goal-directed hand and mouth movements) of the ventral premotor cortex of the macaque monkey [3]. Neurons in F5 discharged not only during the execution of a certain grasping movement, but also when the monkey observed the

experimenter producing the same action. The core areas of the postulated observation–execution matching system [4], or the mirror neuron system (MNS), are areas F5, PF and PG (PFG), and AIP of the macaque brain. The first evidence suggesting that action perception and execution are interconnected was shown on the basis of *motor resonance*, partial activation of motor cortices without movement production measured with non-invasive methods such as EEG, MEG or fMRI (e.g. [5]). The first single cell recording of mirror neurons in humans was made on patients with medically intractable epilepsy [6]. However, the measuring sites were not chosen for academic, but for medical purposes, so they did not contain crucial areas of interest homologous to monkey’s F5 and related circuitry (such as Broca’s area). Interestingly, connections between visual and motor areas are not restricted to what has been identified as the MNS.

As mentioned above, the core of the MNS consists of premotor and posterior areas, in which mirror neurons were discovered. However, important parts of the whole machinery are also visual areas that project information to mirror neurons. According to [7], the flow of information between visual and mirror areas is bidirectional, rather than unidirectional (from visual to motor areas). The authors have proven their theory on the basis of computational model briefly described in Sec. I-B.

One of the major areas projecting to the MNS is the superior temporal sulcus (STS), which is sensitive to a large variety of biological movements, but lacks multi-modal properties displayed by mirror neurons. An interesting property of STS is that it contains many neurons that are sensitive to viewpoint from which the object is observed (e.g. front view, side view, etc.) in its posterior part (STSp), but also neurons that are invariant to it, in anterior part (STSa) [8]. A part of the focus area F5 (F5c) is connected with STSp through PFG forming a perspective variant path. Another part of F5 (F5a) is also connected with STSa through AIP, forming an invariant path emphasizing the actor and the object acted upon, rather than the viewpoint from which it is observed [9]. More possible sources of visual information for area F5 were identified [10], suggesting the involvement of the prefrontal area BA12.

In addition, view-variant and invariant firing properties were also recently discovered in area F5 [11]. In the experiment, monkeys observed grasping actions filmed from three different perspectives, namely the self-observing view ( $0^\circ$ ), the side view ( $90^\circ$ ), and the opposite view ( $180^\circ$ ). Variant and invariant mirror neurons were found in roughly 3:1 ratio. In this paper, we focus on variant and invariant neurons in visual and motor areas, which have (to our knowledge) not yet been addressed in the related computational modeling literature.

## B. Computational models

The discovery of mirror neurons gave rise to various computational models, mainly based on artificial neural networks. Computational models of MNS are considered a powerful tool for explaining the mirror neuron function and emergence [12]. Most of the models aim at capturing the actual neural circuitry, by having components that directly represent particular parts of the monkey’s brain, like FARS, MNS1 and MNS2, MSI, and other [13]. On the other hand, there are models from the field of cognitive robotics which attempt to model the emergence of mirror neurons, such as the RNNPB model [14], which combines temporal error backpropagation learning and the self-organized formation of special codes (parametric biases) that are able to trigger specific behavior of the network without an actual sensory input. These self-organized parametric biases can be considered analogous to mirror neurons. Our model roughly models brain areas at certain level of abstraction but also aims to allow the robot (simulated iCub) to associate the observed action with actions in its own motor repertoire. This mechanism will also allow the robot to make categorical judgments about the observed movement, and to a certain degree “understand” this movement.

A different approach to exploring and modeling mirror neurons was taken by Tessitore et al. [7] who aimed to show the benefit of the bidirectional flow of information between visual and motor areas. Their main assumption is that mirror neurons facilitate action recognition and control processes, since they provide a simplified motor representation that narrows a wide search space of the visual input. Their model represents a mapping function from visual representation (an image of the hand during grasping action) to motor representation (created with a special recording glove). An interesting property of this model is that it directly solves the problem of translation of the perspective, i.e. from the observer to oneself. Most of the classic MNS models, such as those mentioned above, do not address this property, but rather assume some kind of visual preprocessing (in STS) that leads to perspective invariance. However, as suggested by recent empirical findings [11], mirror neurons might be tuned to different perspectives as well as neurons in STSp. Therefore, the perspective information should be encompassed by a computational model of mirror neurons as well. In our modeling, we aim at accounting for the existence of view-dependency of neurons in both STS and F5 as a possible outcome of their bidirectional connectivity.

## II. ROBOTIC MNS MODEL

Our robotic MNS model (Fig. 1) consists of several modules: the core and the topmost part is the mirror neuron circuit itself, which is fed with data from low-level (executive) modules. From the information-flow and neural network type point of view we distinguish three rather than two levels. At the lowest level there are executive modules, namely the motor executive module, feeding sequential motor information like the joint angles to F5c, and the visual module, which provides sequential visual information to STSp (encompassing the observation of another robot producing the movement). We assume that sensory-motor links are established between higher level representations, rather than directly between low-level representations of the movement as a temporal sequence of the robot arm’s state. At the middle level there are two

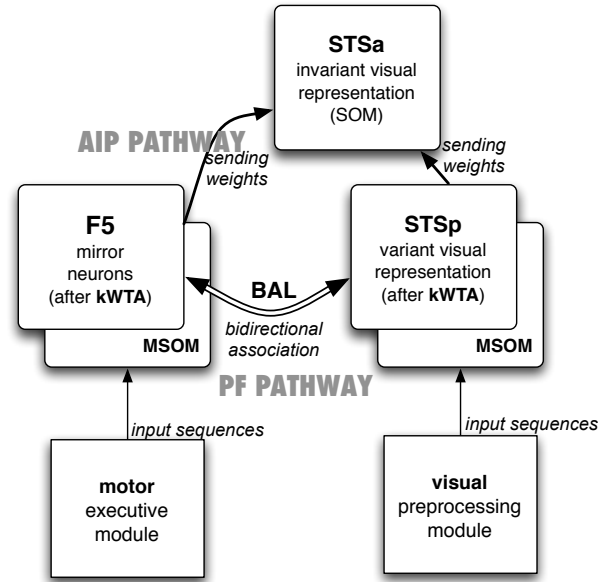


Fig. 1: The sketch of our robotic MSN model.

modules that process the low-level motor and visual information, and form high-level representation of movement in F5 and STSp, respectively.

The topmost part of the model includes a three-layer network, as an abstraction of the F5c–PF–STSp circuit, linking (yet) invariant motor information (area F5) with variant perceptual information (STSp) via the parietal area (PF) in a bidirectional fashion, and the F5a–AIP–STSa circuit, linking motor information with invariant anterior part of the STS. The latter circuit is a self-organizing map (SOM) [15], representing the STSa area, where neurons with various degree of invariance emerge. In the present state we do not divide F5 into F5c and F5a. Neither do we explicitly model the intermediate areas PF and F5. Area PF forms a hidden layer of neurons in BAL network, which we do not access directly, hence its activation is self-organized by the network behavior. AIP pathway is represented by the F5–to–STSa part of the model.

For experiments we chose the freely available simulator [16] of the iCub robot [17] that is considered to be one of the most “accurate” humanoid robots. Designed to resemble a 2.5-year-old child, endowed with 53 degrees of freedom (DoF), movable eyes with color cameras, and various other sensors, the platform provides a very accurate model of an actual child’s body and effectors. For generating the grasping sequences, the simulated iCub was trained using continuous reinforcement learning algorithm, CACLA [18]. An example of such a module previously implemented can be found in [19]. The iCub learned to perform three types of grasp (shown in Fig. 2) related to objects of various sizes and shapes [20].

The higher areas, F5 and STS, are both implemented as MSOM [21], the self-organizing maps<sup>1</sup> that can process

<sup>1</sup>We consider topographic maps as a ubiquitous organizing principle in the brain [22]. Although it is not known whether STS (STSp) and F5 (F5c) areas are also organized this way, we chose the map organization also because it lends itself nicely to providing compact distributed representations as described in Experiment 2.

sequential data. We assume, in line with our motivation mentioned above, that the bidirectional association between these two areas must be established. We approach this using a supervised bidirectional learning algorithm, which we developed on the basis of biologically plausible GeneRec algorithm [23].

In the process of acquiring the whole MNS functionality the robot first learns to produce the three grasps. The information from the motor module is processed with the higher level F5c module (MSOM, Sec. III-A) and gets organized on the resulting map as clusters of instances of the same movements. During the production of the movement, the motor information and the visual information from the self-observation perspective gets associated bidirectionally using the BAL algorithm (Sec. III-B). At the same time, we assume that the robot observes another robot producing the same actions and creates visual representations of those actions from different perspectives (self,  $90^\circ$ ,  $180^\circ$ , and  $270^\circ$ ) in STSp and associates them with the motor representations as well (using BAL). Then, if the robot observes an action from various perspectives, the motor representation of the action is triggered as well. This motor representation, which is basically invariant then projects to STSa module together with visual information from STSp. In line with [7], motor information helps to form the view-independent representations in the visual areas, thus forming categorical representations potentially used for distinguishing and understanding of the movement as such.

### III. BUILDING BLOCKS OF OUR MODEL

#### A. Merge Self-Organizing Map

Since the MSOM model [21] is not widely known, we describe it briefly here. MSOM is based on the well-known Kohonen's self-organizing map but it has recurrent architecture, so it can be used for self-organization of sequential data. Hence, each neuron  $i \in \{1, 2, \dots, N\}$  in the map has two weight vectors associated with it: (1)  $\mathbf{w}_i^{\text{inp}} \in \mathcal{R}^n$  - linked with an  $n$ -dimensional input vector  $\mathbf{s}(t)$  feeding the network at time  $t$ , and (2)  $\mathbf{w}_i^{\text{ctx}} \in \mathcal{R}^n$  - linked with the so-called context descriptor  $\mathbf{q}(t)$  specified below. The output of unit  $i$  at time  $t$  is computed as  $y_i(t) = \exp(-d_i(t))$ , where

$$d_i(t) = (1 - \alpha) \cdot \|\mathbf{s}(t) - \mathbf{w}_i^{\text{inp}}(t)\|^2 + \alpha \cdot \|\mathbf{q}(t) - \mathbf{w}_i^{\text{ctx}}(t)\|^2 \quad (1)$$

Parameter  $0 < \alpha < 1$  trades off the effect of the context and the current input on the neuron's profile and  $\|\cdot\|$  denotes the Euclidean norm. The context descriptor is calculated based on the affine combination of the weight vectors of the previous best matching unit ('winner')  $b(t-1) = \arg \min_i \{d_i(t-1)\}$ ,

$$\mathbf{q}(t) = (1 - \beta) \cdot \mathbf{w}_{b(t-1)}^{\text{inp}}(t) + \beta \cdot \mathbf{w}_{b(t-1)}^{\text{ctx}}(t) \quad (2)$$

where parameter  $0 < \beta < 1$  trades off the impact of the context and the current input on the context descriptor. The training sequences are presented in natural order, one input vector a time, and in each step both weight vectors are updated using the same form of Hebbian rule:

$$\Delta \mathbf{w}_i^{\text{inp}}(t) = \gamma \cdot h_{ib} \cdot (\mathbf{s}(t) - \mathbf{w}_i^{\text{inp}}(t)), \quad (3)$$

$$\Delta \mathbf{w}_i^{\text{ctx}}(t) = \gamma \cdot h_{ib} \cdot (\mathbf{q}(t) - \mathbf{w}_i^{\text{ctx}}(t)), \quad (4)$$

where  $b$  is the winner index at time  $t$  and  $0 < \gamma < 1$  is the learning rate. Neighborhood function  $h_{ib}$  is a Gaussian (of width  $\sigma$ ) on the distance  $d(i, k)$  of units  $i$  and  $b$

in the map:  $h_{ib} = \exp(-d(i, b)^2/\sigma^2)$ . The 'neighborhood width',  $\sigma$ , linearly decreases in time to allow for forming topographic representation of input sequences. As a result, the units (i.e. their responsiveness) get organized according to sequence characteristics, biased towards their suffixes (most recent inputs).

#### B. Bidirectional Activation-based Learning Algorithm

Once the MSOM have been trained, they can generate map outputs (as described in Experiment 1) that can serve as patterns to be associated. For learning the association between sensory and motor representations, we use a three-layer bidirectional perceptron trained using our Bidirectional Activation-based Learning algorithm (BAL) [24].

The main purpose of BAL is to establish a bidirectional mapping between two domains. BAL was inspired by generalized recirculation (GeneRec) algorithm [23] that had been designed as a biologically plausible alternative to standard error backpropagation. In GeneRec, the learning is based on activation propagation in both directions (i.e. input-to-output, as well as output-to-input directions), and under certain circumstances, it has been shown to approximate the error derivatives computed in error backpropagation network (without having to propagate the error). BAL shares with GeneRec the phase-based activations but differs from it in two features. First, BAL employs unit activation propagation, allowing the completely bidirectional associations to be established (GeneRec basically focuses on input-output mapping). By this we mean that not only output can be evoked by input presentation, but also input can be evoked by output presentation.<sup>2</sup> Second, in BAL we do not let the activations to settle but compute them in one step (GeneRec was related to earlier Almeida-Pineda recurrent backpropagation network model whose core feature is the settling of unit activations before weight adaptation).

Neurons in BAL are perceptron units with standard (unipolar) sigmoid activation function. Forward (sensory-to-motor) activation is denoted with subscript F, backward (motor-to-sensory) activation is denoted with subscript B.<sup>3</sup> Let the activations of sensory (visual) units be denoted  $\mathbf{v}$ , and motor units  $\mathbf{m}$ . The hidden units have activations  $\mathbf{h}$ . Then during the forward pass, the sensory units are clamped to  $\mathbf{v}^F$  and we get the activations  $\mathbf{v}^F \rightarrow \mathbf{h}^F \rightarrow \mathbf{m}^F$ . During the backward pass, the motor units are clamped to  $\mathbf{m}^B$  and we get the activations  $\mathbf{m}^B \rightarrow \mathbf{h}^B \rightarrow \mathbf{v}^B$ .

The mechanism of weights update partially matches that of GeneRec. Each weight in BAL network (i.e. belonging to one of the four weight matrices) is updated using the same learning mechanism (unlike GeneRec), according to which the weight difference is proportional to the product of the presynaptic (sending) unit activation  $a_i$  and the difference of postsynaptic (receiving) unit activations  $a_j$ , corresponding to two activation phases (F and B, in particular order). Specifically, weights in

<sup>2</sup>Actually, now the input/output distinction loses its meaning, because we deal with bidirectional associations between two different (sensory and motor) domains where each domain can serve as input or output.

<sup>3</sup>O'Reilly uses minus and plus phases that correspond to our F and B phases. However, since our model is completely bidirectional i.e. both output and input units can be clamped, we find it more convenient not to follow the notation in [23].

**v-to-m** direction (corresponding to **h** and **m** units, respectively) are updated as

$$\Delta w_{ij}^F = \lambda \cdot a_i^F (a_j^B - a_j^F) \quad (5)$$

where  $\lambda$  is the learning rate. Analogically, the weights in **m-to-v** direction (corresponding to **h** and **v** units, respectively) are updated as

$$\Delta w_{ij}^B = \lambda \cdot a_i^B (a_j^F - a_j^B) \quad (6)$$

All units have trainable thresholds (biases) that are updated in a similar way as weights (being fed with a constant input 1).

#### IV. RESULTS

We present results from two experiments. Experiment 1 encompasses processing of visual (preprocessed Cartesian coordinates) and motor (joint angles) data taken from the trained iCub during grasping an object. In this task, the data are self-organized to high-level topographic representations using the MSOM model. In Experiment 2, we form the association between the two maps using the BAL algorithm. First, we focus on learning the associations between various instances of these movements and their visual representation from the self-observing view, subsequently we present results also for associations between all perspectives.

##### A. Experiment 1: self-organization of sensory and motor inputs

For training MSOMs, we first needed to generate the input data. Both sensory and motor sequences were collected from the simulated iCub robot that had been trained for three types of grasp (power, side and precision grasp) using its right arm [20]. These grasps (shown in Fig. 2) were generated, with 10 instances per category, in such a way that individual trajectories slightly differed from one another (which was achieved by adding small perturbations to arm joints during the motion execution).

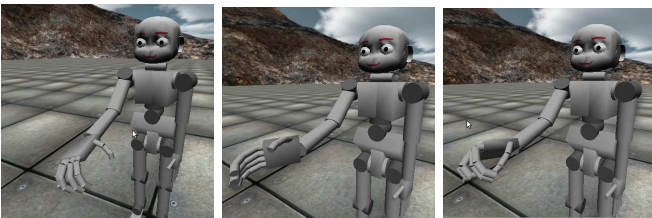


Fig. 2: Examples of three grasp types from the observer's perspective. Left to right: power grasp, side grasp and precision grasp.

1) *Collecting the motor and visual data from iCub:* The motor representations are based on proprioceptive information provided by all joint values from 16 DoF in robot's right arm which were stored during the motor execution, i.e. input vectors for motor MSOM  $\mathbf{s}_m \in \mathcal{R}^{16}$ . These values are given in degrees, and so prior to storing them we rescaled them to interval  $\langle -1, 1 \rangle$ , independently for each DoF. The corresponding sensory representations are merely visual, provided by robot's camera in its right eye (for simplicity, we used monocular information). Visual representations were generated for the

corresponding self-execution (self-observing perspective). The visual information was taken in the form of 3D coordinates of all 16 arm joints (48 values), plus 3D coordinates of four finger tips (which turned out to be useful), amounting to 60 coordinates in total (in simulator's world reference frame). These were then projected onto the right camera, yielding 2D coordinates, and hence input vectors  $\mathbf{s}_v \in \mathcal{R}^{40}$ . As in case of motor data, the values were rescaled to  $\langle -1, 1 \rangle$ , independently for each coordinate. To generate visual representations for other perspectives (90°, 180°, and 270°), not directly available from iCub simulator, we used self-observed trajectories (0°) and rotated them correspondingly using appropriate mathematical apparatus. Afterwards, the trajectories were projected onto 2D retina and rescaled.

2) *Finding optimal maps:* In order to obtain map representations, we searched for optimal MSOM parameters. We aimed at getting the map that would optimally distribute its resources (units) for best discrimination of input data. Following the methods from our previous work [25], we calculated three quantitative measures: (1) winner discrimination (WD) returns the proportion of different winners (out of all units) at the end of training; (2) entropy (Ent) evaluates how often various units become winners, so the highest entropy means most balanced unit participation in the competition process; (3) quantization error (QE) calculates the average error at the unit as a result of quantization process. To get the best MSOMs, we systematically varied parameters  $\alpha$  (eq. 1) and  $\beta$  (eq. 2) in the interval (0,1) and selected the configuration with highest WD and Ent and possibly minimal QE. As a result, we chose  $\alpha_v = \alpha_m = 0.3$ ,  $\beta_v = 0.7$ , and  $\beta_m = 0.5$ .

Using these parameters, we trained the MSOMs and evaluated winner hits (i.e. the number of times the particular unit became the winner), for three categories of grasp type for both motor (Fig. 3a) and visual dataset (Fig. 3b), and additionally for four perspectives for the visual dataset (Fig. 3c). Topographic organization of unit's sensitivity is evident in all cases. For visual map, the organization on a coarse level is arranged according to the perspectives, and on a more fine-grained level according to the grasp types. Although some units never became winners, they participated in distributed map representations as well. Topographic order reflects the natural separability of classes (types of grasps) both in terms of their motor and visual features. Visual maps reveal that perspective is a more strongly distinguishing parameter than the type of grasp.

3) *Generating map output responses:* In line with our modeling assumptions, we considered the map responses in the form of distributed representations. In biological networks, these are typically achieved by lateral inhibition, but as a computational shortcut, we used the  $k$ -WTA (winner-take-all) mechanism, similar to the one described in [26]. This mechanism preselects  $k$  maximally responding units (i.e. according to sorted  $y_i$  activations) and resets the remaining units to zero. We used binarization also in order to facilitate the training and to simplify the assessment of network performance.

##### B. Experiment 2: learning bidirectional associations

In this experiment we created a two-phase learning design in order to train the BAL network representing the PF pathway

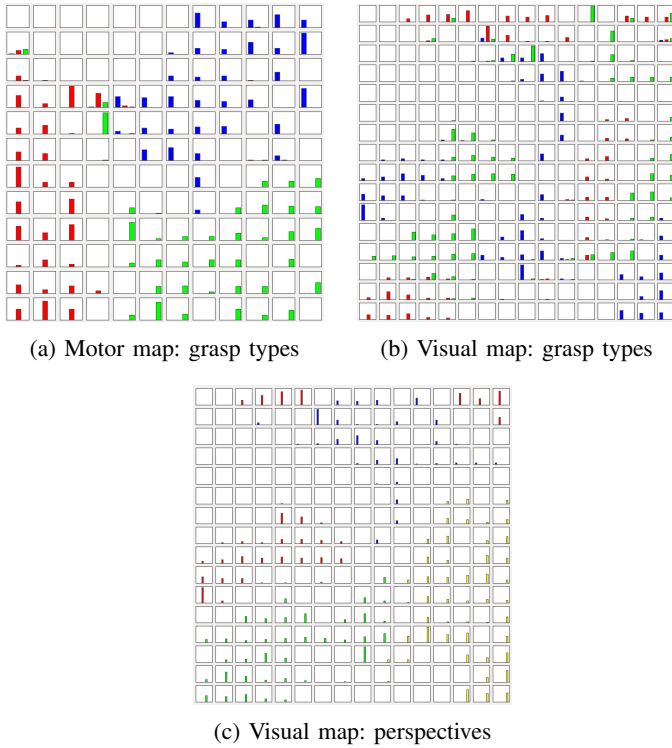


Fig. 3: Examples of the trained motor and visual maps.

between STS and F5. In phase 1, the agent associates its own movements with their appearance on the basis of high-level representations from MSOM binarized using the  $k$ -WTA mechanism. In phase 2, the agent forms bidirectional associations also with the movement seen from the other perspectives. Here we use a sort of “scenario-based shortcut”. The robot first produces the self movement, while observing its own arm. Right after it, while the generated motor pattern is assumed to be still residually active, the robot observes the same movement from another perspective (as if it was playing an educational game with its parent). It is known that parents often imitate children’s immediate behavior providing them with something like a mirror, which may explain how mirror neurons could emerge as a product of associative learning [27].

In testing the map responses, the output of each unit is considered correct if it lies in the correct half of the  $(0, 1)$  interval. For assessing the model accuracy, we used three quantitative measures (separately for F and B directions): (1) mean squared error (MSE) per output neuron, (2) bit success measure (bitSucc), which is the proportion of units matching their target (perfect match equals one), and (3) pattern success (patSucc), which indicates the proportion of output patterns that completely match targets.

We examined various sizes of the trained MSOMs and various numbers of  $k$  positive units for  $k$ -WTA binarization. We experimented with  $k$ , the free parameter that affects the variability of map responses (as distributed patterns of activity) to different inputs, as well as with the size of both maps. Based on these experiments we decided to use visual maps with  $16 \times 16$  units and motor maps with  $12 \times 12$  units both

TABLE I: BAL performance in two learning phases (50 nets).

measure	phase 1		phase 2	
	F	B	F	B
MSE	$0.0 \pm 0.0$	$0.086 \pm 0.003$	$0.002 \pm 0.001$	$0.045 \pm 0.004$
patSucc	$0.999 \pm 0.007$	$0.985 \pm 0.025$	$0.006 \pm 0.005$	$0.495 \pm 0.031$
bitSucc	$1.0 \pm 0.0$	$1.0 \pm 0.0$	$0.906 \pm 0.003$	$0.947 \pm 0.005$

binarized using  $k_m = 16$ . The BAL network had 196–160–144 units with randomly initialized weights from  $(-0.1; 0.1)$  and  $\lambda = 0.2$ . Results from 50 networks after two training phases are displayed in Table I. Fig. 4 displays the network performance over time in phase 1 (800 epochs) and phase 2 (2000 epochs).

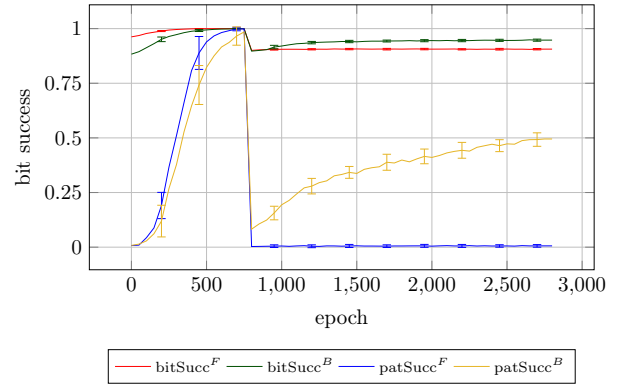


Fig. 4: BAL performance in two learning phases (50 nets).

The results from phase 1 of learning indicate that BAL algorithm is able to form error-free associations between visual and motor representations. Regarding phase 2, it is clear that the task of bidirectional association of ambiguous data (1-to-4 associations) cannot be accomplished in one direction (compare  $\text{patSucc}^F$  and  $\text{patSucc}^B$ ). High bitSucc (up to  $\approx 95\%$ ) indicates that the network matches the desired outcome (at least in  $\mathbf{v}$ -to- $\mathbf{m}$  direction). The 52% success of the reconstruction of the whole motor patterns (i.e. 100% bitSucc) does not necessarily mean that the network performs badly. Combined with high bitSucc and on the basis of closer observation we noticed that the network only makes small errors in this direction. Hence, we can conclude that any visual representation of a particular movement will trigger a proper motor representation of this movement, representing the role of mirror neuron activity. The motor information activated on the basis of the visual input can be further used to facilitate the process of forming invariant representation of the movement in STSa.

## V. DISCUSSION

We presented pilot results directed toward our model of the core mirror neuron system that connects visual representations (STS) with motor representations (F5). In our approach, we were inspired by empirical findings showing that in STS as well as F5, most of the neurons are perspective-dependent, and that this may be the lowest level at which sensory-motor relationships could be established. Perspective invariance emerged

on the basis of local interaction might on the other hand serve for final categorical response of the whole system.

For collecting the sensory and motor data, we used simulated iCub robot that had been trained to reach for and grasp an object with its right hand. In the first place, we have shown how high-level sensory and motor representations could be formed, using recurrent self-organizing maps (MSOM).

Next, we presented our bidirectional activation-based algorithm (BAL) that guides the learning of bidirectional associations between sensory and motor representations. We have shown that using BAL motor patterns can be successfully retrieved based on visual data from various perspectives. Subsequently we will require the motor code to be involved in building perspective invariant representation of the action in STSa. To achieve this, we will add a SOM-based learning mechanism which will associate visual representations from STSp, which are clustered strongly according to the viewpoint, with motor representations from F5, clustered according to the grasp type. Our preliminary results and observations indicate, that motor information helps to re-organize the STSp representations to form major clusters according to the grasp types rather than perspectives, suggesting a good direction towards perspective-invariant representations.

Last but not least, one of the assumptions of our model is the graded degree of invariance of both visual and motor neurons. This appears consistent with empirical evidence when it comes to STS [28], and recent evidence [11] points out that a similar principle could apply to F5. In our model, it is a challenge to achieve graded perspective (or grasp type) invariance in a self-organized manner without prespecifying which neurons should become invariant to which degree. As mentioned in [8], at least in the visual system (STS area), the invariance is built incrementally, possibly by pooling the responses of lower-level (less invariant) units toward higher-level (more invariant) units, eventually leading to completely invariant (categorical) representations. The motor system might be built in an analogical way.

#### ACKNOWLEDGMENT

This work was supported by grants 1/0439/11 and 1/0503/13 from Slovak Grant Agency for Science, and grant UK/631/2013 (K.R.). We thank Lukáš Zdechovan for providing the visual and motor sequences from the trained iCub.

#### REFERENCES

- [1] T. Ziemke, "Are robots embodied," in *First International Workshop on Epigenetic Robotics*, vol. 85, 2001.
- [2] G. Rizzolatti, L. Fogassi, and V. Gallese, "Neurophysiological mechanisms underlying the understanding and imitation of action," *Nature Reviews Neuroscience*, vol. 2, pp. 661–670, 2001.
- [3] G. Pellegrino, L. Fadiga, L. Fogassi, V. Gallese, and G. Rizzolatti, "Understanding motor events: a neurophysiological study," *Experimental Brain Research*, vol. 91, no. 1, pp. 176–180, 1992.
- [4] G. Rizzolatti and C. Sinigaglia, "The functional role of the parieto-frontal mirror circuit: interpretations and misinterpretations," *Nature Reviews Neuroscience*, vol. 11, no. 4, pp. 264–74, 2010.
- [5] L. Oberman and V. Ramachandran, "The simulating social mind: The role of the mirror neuron system and simulation in the social and communicative deficits of autism spectrum disorders," *Psychological Bulletin*, vol. 133, no. 2, p. 310, 2007.
- [6] R. Mukamel, A. Ekstrom, J. Kaplan, M. Iacoboni, and I. Fried, "Single-neuron responses in humans during execution and observation of actions," *Current Biology*, vol. 20, no. 8, pp. R353–R354, 2010.
- [7] G. Tessitore, R. Prevede, E. Catanzariti, and G. Tamburrini, "From motor to sensory processing in mirror neuron computational modelling," *Biological Cybernetics*, vol. 103, no. 6, pp. 471–485, 2010.
- [8] T. Jellema and D. Perrett, "Neural representations of perceived bodily actions using a categorical frame of reference," *Neuropsychologia*, vol. 44, pp. 1535–1546, 2006.
- [9] K. Nelissen, E. Borra, M. Gerbella, S. Rozzi, G. Luppino, W. Vanduffel, G. Rizzolatti, and G. A. Orban, "Action observation circuits in the macaque monkey cortex," *The Journal of Neuroscience*, vol. 31, no. 10, pp. 3743–3756, 2011.
- [10] E. Borra and K. S. Rockland, "Projections to early visual areas V1 and V2 in the calcarine fissure from parietal association areas in the macaque," *Frontiers in Neuroanatomy*, vol. 5, 2011.
- [11] V. Caggiano, L. Fogassi, G. Rizzolatti, J. K. Pomper, P. Thier, M. A. Giese, and A. Casile, "View-based encoding of actions in mirror neurons of area f5 in macaque premotor cortex," *Current Biology*, vol. 21, no. 2, pp. 144–148, 2011.
- [12] E. Oztop, M. Kawato, and M. Arbib, "Mirror neurons: Functions, mechanisms and models," *Neuroscience Letters*, vol. 540, pp. 43–55, 2013.
- [13] —, "Mirror neurons and imitation: A computationally guided review," *Neural Networks*, vol. 19, no. 3, pp. 254–271, 2006.
- [14] J. Tani, M. Ito, and Y. Sugita, "Self-organization of distributedly represented multiple behavior schemata in a mirror system: reviews of robot experiments using RNNPB," *Neural Networks*, vol. 17, no. 8–9, pp. 1273–1289, 2004.
- [15] T. Kohonen, *Self-organizing Maps*. Springer, 1997.
- [16] V. Tikhonoff *et al.*, "An open-source simulator for cognitive robotics research: The prototype of the iCub humanoid robot simulator," in *Proceedings of the 8th Workshop on Performance Metrics for Intelligent Systems*. ACM, 2008, pp. 57–61.
- [17] G. Metta, G. Sandini, D. Vernon, L. Natale, and F. Nori, "The iCub humanoid robot: an open platform for research in embodied cognition," in *Proceedings of the 8th Workshop on Performance Metrics for Intelligent Systems*. ACM, 2008, pp. 50–56.
- [18] H. van Hasselt, "Reinforcement learning in continuous state and action spaces," in *Reinforcement Learning: State of the Art*, M. Wiering and M. van Otterlo, Eds. Berlin: Springer, 2012, pp. 207–251.
- [19] I. Farkaš, T. Malík, and K. Rebrová, "Grounding the meanings in sensorimotor behavior using reinforcement learning," *Frontiers in Neuroinformatics*, vol. 6, no. 1, 2012.
- [20] L. Zdechovan, "Modeling the object grasping using the neural networks and iCub robotic simulator (in Slovak)," Master's thesis, Comenius University in Bratislava, 2012.
- [21] M. Strickert and B. Hammer, "Merge SOM for temporal data," *Neurocomputing*, vol. 64, pp. 39–71, 2005.
- [22] J.-P. Thivierge and G. Marcus, "The topographic brain: from neural connectivity to cognition," *Trends in Neurosciences*, vol. 30, no. 6, pp. 251–259, 2007.
- [23] R. O'Reilly, "Biologically plausible error-driven learning using local activation differences: The generalized recirculation algorithm," *Neural Computation*, vol. 8, no. 5, pp. 895–938, 1996.
- [24] I. Farkaš and K. Rebrová, "Bidirectional activation-based neural network learning algorithm," in *Proceedings of the International Conference on Artificial Neural Networks (ICANN)*, Sofia, Bulgaria, 2013.
- [25] P. Vančo and I. Farkaš, "Experimental comparison of recursive self-organizing maps for processing tree-structured data," *Neurocomputing*, vol. 73, no. 7–9, pp. 1362–1375, 2010.
- [26] R. O'Reilly, Y. Munakata, M. Frank, T. Hazy, and Contributors, *Computational Cognitive Neuroscience*, 2nd ed. Wiki book, 2012.
- [27] C. Heyes, "Where do mirror neurons come from?" *Neuroscience and Biobehavioral Reviews*, vol. 34, no. 4, pp. 575–83, 2010.
- [28] D. Perrett *et al.*, "Viewer-centred and object-centred coding of heads in the macaque temporal cortex," *Experimental Brain Research*, vol. 86, no. 1, pp. 159–173, 1991.